$P^+H_A^-$ Charge Recombination Reaction Rate Constant in *Rhodobacter sphaeroides* Reaction Centers Is Independent of the P/P^+ Midpoint Potential†

Chu-Kang Tang, JoAnn C. Williams, Aileen K. W. Taguchi, James P. Allen, and Neal W. Woodbury*

Department of Chemistry and Biochemistry and the Center for the Study of Early Events in Photosynthesis, Arizona State University, Tempe, Arizona 85287-1604

Received February 11, 1999; Revised Manuscript Received April 27, 1999

ABSTRACT: The kinetics of the $P^+H_A^-$ (oxidized donor, reduced bacteriopheophytin acceptor) recombination reaction was measured in a series of reaction center mutants of *Rhodobacter sphaeroides* with altered P/P^+ midpoint potentials between 410 and 765 mV. The time constant for $P^+H_A^-$ recombination was found to range between 14 and 26 ns and was essentially independent of P/P^+ midpoint potential. Previous work has shown that the time constant for initial electron transfer in these mutants at room temperature is also only weakly dependent on the P/P^+ midpoint potential, ranging from about 2.5 ps to about 50 ps. These results, taken together, imply that heterogeneity in the P/P^+ midpoint potential within the reaction center population is not likely the dominant cause of the substantial kinetic complexity observed in the decay of the excited singlet state of P on the picosecond to nanosecond time scale. In addition, the pathway of $P^+H_A^-$ decay appears to be direct or via $P^+B_A^-$ rather than proceeding back through P*, even in the highest-potential mutant, as is evident from the fact that the rate of $P^+H_A^-$ recombination is unaltered by pushing $P^+H_A^-$ much closer to P* in energy. Finally, the midpoint potential independence of the $P^+H_A^-$ recombination rate constant suggests that the slow rate of $P^+H_A^-$ recombination arises from an inherent limitation in the maximum rate of this process rather than because it occurs in the inverted region of a classical Marcus rate vs free energy curve.

The primary energy conversion reaction of photosynthesis is light-powered charge separation in the reaction center. This results in the picosecond time scale formation of two formal charges buried inside the protein, providing the opportunity to study the role of protein conformational heterogeneity and dynamics during both the initial charge separation and subsequent dielectric relaxation processes on time scales as fast as picoseconds. The rapid forward electron-transfer rates, the subsequent solvation by the protein enviroment, and the slow rates of nonproductive recombination of charge-separated intermediates are all critical in maintaining a near unity yield for the initial solar energy conversion pathway.

Figure 1 shows a diagram of all the reaction center cofactors, the pathway of charge separation, and the rate constants of the charge separation and charge recombination reactions that can take place (for reviews see refs *1*−*7*). Initial electron transfer is very rapid, taking place in a few picoseconds to form $P^+H_A^-$ (presumably via $P^+B_A^-$). Subsequent electron transfer to the quinone (Q_A) occurs with a rate constant of about 200 ps. If Q_A is either removed or reduced chemically, $P^+H_A^-$ lives for 10−20 ns before recombining either to the ground state or to the triplet excited state of P (triplet formation occurs with a low yield at room temperature). During the lifetime of $P^+H_A^-$, a weak fluorescence signal is observed due to the small equilibrium population of P*. The kinetics of this recombination reaction are important as they determine the yield for electron transfer to the quinone and indirectly affect the rate of excited singlet state decay due to back reactions between $P^+H_A^-$ and P* when electron transfer to the quinone is blocked.

There is an extensive literature of P* fluorescence decay measurements both from wild-type bacterial reaction centers and from mutants with altered P/P^+ midpoint potentials (*1*, *8*−*15*). The hallmark of the excited singlet state decay is its complexity, with component lifetimes from the time scale of initial electron transfer (a few picoseconds) out to many nanoseconds. A qualitatively similar multiexponential fluorescence decay has also been observed in photosystem II of plants (*16*, *17*), suggesting that this is a general property of reaction centers. It is likely that on the picosecond to several hundred picosecond time scale this is due to a mixture of both static conformational heterogeneity in the reaction center population and solvation dynamics of the charge-separated state by the surrounding protein (*11*, *13*−*15*, *18*−*21*). On the nanosecond time scale, solvation dynamics altering the free energy difference between the charge-separated and fluorescent excited state appears to play the major role in the complexity of the excited singlet state decay (*9*−*11*, *13*, *18*−*21*). This concept is illustrated in Figure 2. As solvation of the charge-separated state occurs by the surrounding protein, the free energy drops relative to the excited state and the equilibrium excited-state population decreases. This provides a nanosecond time scale window for observing the energetic changes in the charge-separated state due to protein dynamics.

† This work was supported by Grants MCB-9513457-004 and MCB-9817388 from the National Science Foundation and 9901753 from the U.S. Department of Agriculture. This is publication 407 from the Arizona State University Center for the Study of Early Events in Photosynthesis.

* Corresponding author: E-mail NWoodbury@ASU.EDU.

10.1021/bi990346q CCC: $18.00
Published on Web 06/11/1999

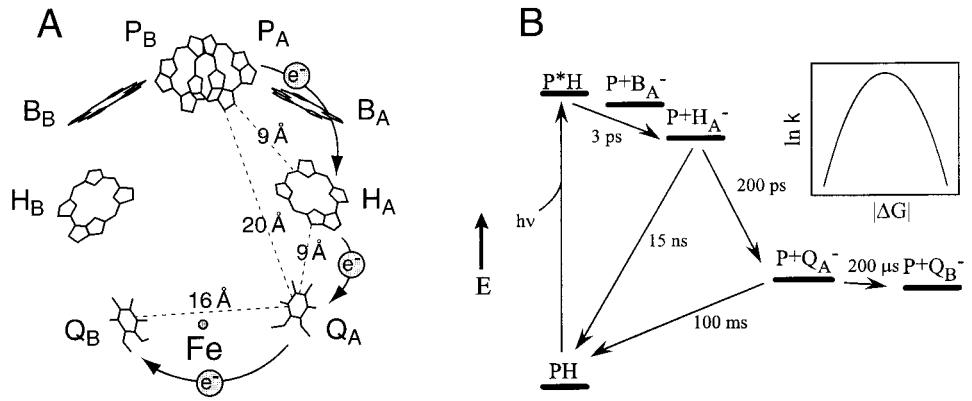

FIGURE 1: (A) Schematic diagram of the reaction center cofactors from *Rhodobacter sphaeroides*. Structural information was taken from published reaction center X-ray structures (*38*−*44*). The approximate edge-to-edge distances between the cofactors are shown. P is the pair of bacteriochlorophylls that makes up the initial electron donor, B_A and B_B are monomer bacteriochlorophylls, H_A and H_B are bacteriopheophytins, and Q_A and Q_B are both ubiquinones. (B) Energy and kinetic diagram of the excited and charge-separated states involved in the electron-transfer reactions at 295 K. Times shown are the observed rate constants rather than model-dependent rate constants (for example, one observes that P* decays and $P^+H_A^-$ forms in about 3 ps, though $P^+B_A^-$ is likely transiently involved). Both forward electron-transfer rate constants and recombination rate constants are shown. Recombination from $P^+H_A^-$ in the absence of electron transfer to Q_A (which is shown as an arrow to the ground state with a time constant of 15 ns) can actually occur either directly or via the triplet state of P, ^3P (not shown). At room temperature, the singlet recombination route directly to the ground state dominates. The inset shows the shape of the dependence of the natural log of the electron-transfer rate constant on the free energy difference between the charge-separated state and the ground state, according to the Marcus expression in the Discussion. This expression peaks where $|\Delta G| = \lambda$.

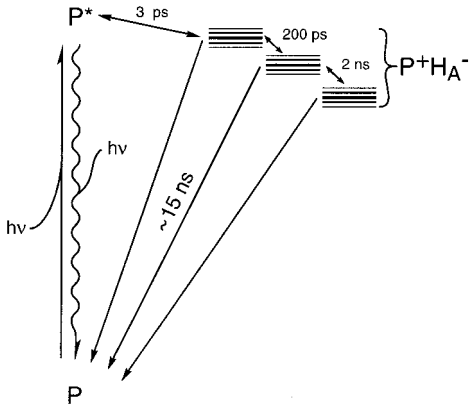

FIGURE 2: Model explaining the complex fluorescence decay from bacterial reaction centers. P* fluorescence kinetics are determined by the kinetics of the initial electron transfer (the prompt fluorescence) and by fluorescence due to equilibration between P* and $P^+H_A^-$ on longer time scales. When electron transfer from H_A to Q_A is blocked by removal of Q_A, $P^+H_A^-$ lives for about 15 ns, and a complex fluorescence decay time course is observed with many time constants from picoseconds to nanoseconds. This kinetic complexity at early time likely arises from two sources: static heterogeneity in the rate constants for forward electron transfer and recombination due to a distribution in $P^+H_A^-$ relative free energies (shown as a series of energy levels for each of the $P^+H_A^-$ conformational intermediates) and time-dependent changes in the relative free energy of $P^+H_A^-$ (represented here by two successive conformational relaxations with lifetimes of 200 ps and 2 ns). The latter has an effect on the fluorescence amplitude because as the protein environment moves to accommodate the charge-separated state, the free energy drops with time and therefore $P^+H_A^-$ becomes thermodynamically farther and farther from P*. Thus, with time, the equilibrium population of P* decreases and so does the fluorescence intensity.

If the excited singlet state decay kinetics is interpreted in terms of dynamic solvation of the charge-separated state by the surrounding protein, one concludes that after about 100 ps in bacterial reaction centers (after complete equilibration between P* and $P^+H_A^-$), the free energy difference between P* and $P^+H_A^-$ is −120 to −160 meV. During the next several nanoseconds, the relative free energy of $P^+H_A^-$ drops (becomes more negative) by roughly 100 meV as the protein relaxes around the charge-separated state (Figure 2; see also ref *1* for a review).

While it is generally agreed upon that both static and dynamic conformational heterogeneity play a role in the kinetic complexity of early charge-separated reactions, it remains unclear what the origin of the conformational heterogeneity is and exactly what aspects of this conformational heterogeneity are changing on the picosecond and nanosecond time scales. One way to investigate this is by altering parameters involved in electron transfer systematically through mutagenesis and observing the resulting changes in reaction center dynamics on various time scales. In this way, it is possible to estimate what effects natural variations in these parameters will have on the charge separation and recombination (loss) processes.

One mutagenically accessible parameter is the midpoint potential of the initial electron donor of the reaction center, P. A series of *Rhodobacter sphaeroides* reaction center mutations have been constructed that vary this midpoint potential in increments over a roughly 350 mV range. By use of these mutants, it has been shown that the P* to $P^+H_A^-$ forward electron-transfer rate constant ranges from about 2.5 ps to about 50 ps between the lowest and highest potential mutant (*22*). This suggests that moderate heterogeneity in the P/P^+ midpoint potential (±100 mV) is unlikely to cause a change in the initial electron-transfer rate of more than a few fold. In this report, the dependence of the $P^+H_A^-$ recombination rate constant on the relative free energy of this state is explored by using the same set of reaction center mutants. This should provide information about the possible effects of population heterogeneity in the P/P^+ midpoint potential on the recombination rate constant. Some information about the effect of P/P^+ midpoint potential on $P^+H_A^-$ recombination kinetics has been obtained from previous mutants and strain comparisons, and the dependence of the recombination rate constant on driving force is apparently weak (*23*−*25*). In the present work a much more thorough

rate vs P/P^+ midpoint potential dependence is obtained over a much larger range of midpoints.

EXPERIMENTAL PROCEDURES

Bacterial Strains and Reaction Center Preparations. The wild-type and mutant strains of *Rhodobacter sphaeroides* used in this study have been described previously (reviewed in ref *22*). Cells were grown semiaerobically in the dark. Reaction centers were then isolated and suspended in 15 mM Tris-HCl (pH 8), 0.025% lauryl dimethylamine oxide, and 1 mM EDTA as described in refs *26* and *27*. For transient spectroscopic measurements, the quinones were removed (*28*).

Nanosecond Transient Spectroscopy. Absorbance change measurements on the nanosecond time scale were performed on quinone-depleted reaction centers. The probe beam (870 nm) was generated by a continuous-wave (CW) titanium sapphire laser (Lexel Lasers), which was pumped by a 5 W argon ion laser (Lexel Lasers). This beam (about 2 mm in diameter, about 100 μW, and vertically polarized) was passed through a 1 cm sample cell, through an aperture and focused through a 750 nm long-pass filter onto a photodiode with a built-in amplifier (New Focus, model 1801, 3 ns response time). The pump pulse (532 nm) was provided by a doubled Nd−YAG laser (SureLight, Continuum Inc.). For these experiments, 20−40 mJ/pulse was defocused to cover the whole surface of the cuvette (about 2 cm^2). The excitation was from the back surface of the cuvette and the instrument response time (full width at half-maximum) was about 5 ns, as determined by observing the signal from scattered 532 nm light in the sample chamber (shown in Figure 3). The signal was monitored by a fast transient digitizer (Tektronix 7912H with a 750 MHz front end and 512 channels). The digitized transients were then transferred to a computer. The analysis reported here was done using SigmaPlot (Jandel Corp.). All curves were fit to the function $A(t) = a_0 + a_1 \exp(-kt)$, where a_0, a_1, and k were free parameters. No deconvolution was performed in these fits, and the fitting was started near the peak of the transmittance change signal.

RESULTS

The transmittance change kinetics at 870 nm, after excitation by a roughly 5 ns pulse at 532 nm, is shown in Figure 3. Quinone-depleted reaction centers from *Rb. sphaeroides* R-26, *Rb. sphaeroides* wild type, and six different mutants were studied, including the triple mutant LH(M160) + LH(L131) + FH(M197), which has a P/P^+ midpoint potential 260 mV above that of wild type, and HF-(L168), which has a midpoint potential 95 mV below that of wild type (*22*). Quinone-depleted reaction centers were used in order to observe the decay of the $P^+H_A^-$ state due to recombination, rather than forward electron transfer to the quinone. Measurements were performed at 870 nm because this is near the peak of the ground-state absorbance of P. The absorbance band at this wavelength bleaches upon excited state formation (causing an increase in transmittance), remains bleached during charge separation, and then recovers during charge recombination from $P^+H_A^-$ (except in the small population of reaction centers that recombine to the triplet state at this temperature; see below). The wild-type and mutant bleaching decay kinetics are very similar for all

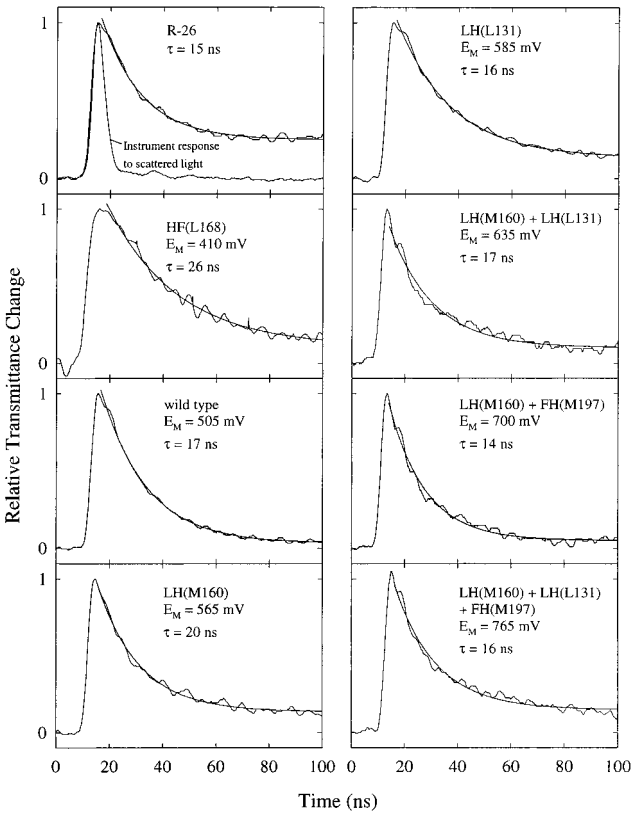

FIGURE 3: Decay of the transmittance change signal at 870 nm from wild-type, strain R-26, and six mutant reaction centers upon excitation at 532 nm with a 5 ns pulse. Mutants are named as follows: LH(L168) is a leucine to histidine change at position 168 of the L subunit of the reaction center. The E_M given for each sample is the measured P/P^+ midpoint potential (*22*). The time course of the excitation pulse (shown in the top left panel) was determined from scattered excitation light from the sample. The solid lines passing through the data represent fits to a single-exponential decay term and a constant term ($a_0 + a_1 e^{-t/\tau}$) without deconvolution of the instrument response function. The decay times resulting from the fit are shown.

mutants except HF(L168), which decays significantly more slowly than wild type. The long-lived transmittance change that remains after 100 ns in all samples has a larger amplitude in some of the mutants than in the wild type.

In addition to $P^+H_A^-$, there are two other states which can be formed that result in bleaching at 870 nm. First, the quinone removal process is not 100% efficient and therefore there is a small (typically 5%) population of reaction centers for which $P^+Q_A^-$ formation occurs. This is one factor that can give rise to a small long-lived bleaching at 870 nm. The other possibility is charge recombination to the triplet state of P, ^3P. In R-26 reaction centers, there is no carotenoid present and the triplet lifetime is microseconds. One can see from Figure 3 that the yield of long-lived signal is roughly 25% of the initial signal in R-26 reaction centers at this temperature, consistent with earlier studies (*3, 8*). Note that the triplet contribution is likely less than this, since the size of the rapidly decaying signal is somewhat shortened due to convolution with the laser pulse and some of the long-lived signal is probably due to a small fraction of reaction centers in which the quinones were not removed. In the other reaction center samples, which contain carotenoids, the triplet state of P decays on the time scale of 20−100 ns (*29, 30*) but presumably has a yield similar to that in R-26. Thus,

the predominant bleaching signal in the traces of Figure 3 should be due to $P^+H_A^-$ recombination to the ground state.

Figure 3 also shows fits of the transmittance change kinetics to a single exponential and a constant term. The fitting was performed from approximately the point where the signal is maximal onward. The decay times (τ) resulting from the exponential decay analyses are shown in each panel and the fitting functions are shown as solid lines running through each of the data traces in Figure 3. The state $P^+H_A^-$ decays with roughly the same overall time constant (17 ± 3 ns) in all of these samples except HF(L168), where the decay time constant is about 50% longer than wild type. Apparently, the $P^+H_A^-$ recombination rate is nearly independent of the P/P^+ midpoint potential, and thus independent of the driving force for recombination, over this range of potentials.

DISCUSSION

$P^+H_A^-$ Does Not Decay through P Even in High-Potential Mutants.* At room temperature in wild-type reaction centers, $P^+H_A^-$ is thought to be on the order of 0.2−0.3 eV lower than P* after dielectric relaxation on the nanosecond time scale. It is therefore unlikely that much of the decay of $P^+H_A^-$ proceeds via P*, given that the inherent time constant for P* decay (in the absence of charge separation) is apparently between 0.2 and 2 ns, depending on which mutant is used for making the estimate (*31*−*33*). In wild type at room temperature, the decay time of $P^+H_A^-$ through P* should be at least 200 ns (the equilibrium constant between P* and $P^+H_A^-$ after a couple of nanoseconds is on the order of 1000, and this multiplied by the inherent decay rate constant for P* gives the overall rate constant for decay of $P^+H_A^-$ via P*). However, raising the P/P^+ potential by 260 mV in the triple mutant (lower right-hand panel of Figure 3) should bring $P^+H_A^-$ nearly isoenergetic with P* and thus P* should become a viable decay route, with a decay rate constant approaching that of P* itself. The fact that a faster decay route did not dominate in the high-potential mutants means that either the intrinsic lifetime of P* in the absence of charge separation in these mutants is many nanoseconds or that raising the P/P^+ midpoint potential by 260 mV does not necessarily raise the standard free energy of $P^+H_A^-$ by the same amount. The latter would be possible either if the mutants also changed the midpoint potential of H_A or if the degree to which the P/P^+ potential was changed in the mutants depended on time given for relaxation of the protein around P^+.

Rate vs Driving Force Dependence of $P^+H_A^-$ Recombination. Since $P^+H_A^-$ recombination apparently does not proceed to an appreciable extent via P* in either the wild-type or mutant reaction centers, it must recombine either directly or via a different intermediate. For direct recombination of $P^+H_A^-$, the fact that the rate is essentially independent of the P/P^+ midpoint potential (and therefore, presumably, the driving force), implies that this reaction is occurring in a region of the rate constant vs driving force relationship that is relatively flat. There are several possible ways that this could come about. In a simple, single vibrational mode theory of electron transfer (*34*), one finds that the dependence of rate on free energy is represented by the term, $\exp[-(\Delta G + \lambda)^2/4\lambda k_B T]$. Here, the negative of the driving force is given by ΔG, the free energy change for the reaction, and the reorganization energy is given by λ. k_B is the Boltzmann constant, and T is temperature. This curve is an inverted parabola (inset, Figure 1). The only region of the curve where the reaction becomes locally independent of driving force is near the peak, where the reorganization energy and the driving force are nearly equal. It is noteworthy that the HF(L168) mutant appears to be significantly slower than the other mutants, and this could represent the upper part of the activated region of the Marcus relationship, though this is speculative. If the classical Marcus relationship is a reasonable description of $P^+H_A^-$ recombination, then $\lambda \cong |\Delta G|$ for wild type (ΔG is a negative number), giving a reorganization energy of about 1.2 eV. For this simple model of the rate vs driving force relationship, if $\lambda \ll |\Delta G|$, then an increase in the driving force for the reaction would result in a decrease in the rate constant. This is the so-called inverted region of the rate vs free energy curve. From the P/P^+ independence of the rate constant in Figure 3, it is clear that $P^+H_A^-$ recombination does not slow with increasing potential, as would be expected in the inverted region of the classical Marcus curve (see below).

More sophisticated electron transfer theories involving multiple vibrational modes coupled to the reaction (*35*) or nuclear tunneling contributions (*36*) have a very similar shape on the steep positive slope of rate constant vs free energy relationship but are governed by a weaker rate constant vs free energy dependence when the driving force is increased past the value that gives the highest rate constant (in the so-called Marcus inverted region). If one of these situations applies to $P^+H_A^-$ recombination, then this reaction may occur in a region well past the peak of the rate constant vs driving force relationship. In this case, it would be difficult to predict the relationship between the magnitude of the driving force and the reorganization energy for the reaction without knowing more about the number and frequencies of the modes involved.

It is also possible that the recombination of $P^+H_A^-$ occurs via $P^+B_A^-$ as a virtual state and that the value of the recombination rate constant is therefore dependent both on the energy between $P^+B_A^-$ and the ground state (which depends on the P/P^+ midpoint potential) and on the energy between $P^+H_A^-$ and $P^+B_A^-$ (which does not depend on the P/P^+ potential). A superexchange mechanism for $P^+H_A^-$ recombination through $P^+B_A^-$ has been suggested previously (see ref *20* and references therein). Consistent with this concept, measurements of $P^+H_A^-$ recombination rates in mutants in which the H_A/H_A^- midpoint potential have been changed do have significantly altered recombination rates. A case in point is the so-called β mutant, in which the introduction of a potential metal ligand in the proper position near H_A results in a bacteriochlorophyll where the bacteriopheophytin resided in wild type (*5*, *37*). In this mutant, the rate of charge recombination increases by more than a factor of 10. Here the relative free energy of $P^+H_A^-$ (now $P^+\beta_A^-$) is increased over that of wild type by ∼100−200 mV, but the free energy of $P^+B_A^-$ is presumably unchanged. Thus, it is likely that recombination occurs through the much more thermodynamically accessible $P^+B_A^-$ state in the mutant. In fact, the recombination may well occur directly via $P^+B_A^-$ in the β mutant, rather than via a superexchange mechanism. The mutants used in the present study to alter the P/P^+ midpoint potential should affect the free energies

of $P^+H_A^-$ and $P^+B_A^-$ equally. Recombination via $P^+B_A^-$ as a virtual state is possible in these mutants but does not completely explain the observation that the $P^+H_A^-$ recombination rate constant is independent of the P/P^+ midpoint potential. Because $P^+B_A^-$ involves P oxidation, its free energy relative to the ground state should change in the mutants studied. This, in turn, should change the overall rate of $P^+H_A^-$ recombination via $P^+B_A^-$, because even in the superexchange model, the relative energy of the virtual state above the ground state is a factor. Here again, one is left to assume that other factors such as multiple vibrational modes or nuclear tunneling flatten out the rate vs free energy curve even well into the so-called inverted region.

Recombination of $P^+H_A^-$ Is Not Slow Due to a Rate Decrease in the Inverted Region. An important aspect of reaction center electron transfer is its very fast forward rate. This rate is necessarily fast because the nonproductive decay of excited or charge-separated states competes with the forward reactions. Clearly it is important to have both fast forward electron transfer and slow recombination. One attractive hypothesis for why $P^+H_A^-$ recombination is slow compared to forward electron transfer is that the recombination occurs far in the inverted region of the rate constant vs driving force curve, where the rate constant should decrease with increased $P^+H_A^-$ relative free energy (increased driving force for recombination) (*6*). Whatever the proper description of the recombination rate dependence on driving force is, it is clear that this dependence is too shallow to support the idea that being far in the classical Marcus inverted region makes the recombination extremely slow.

Role of P/P^+ Midpoint Potential Distributions in the Complex Kinetics of P Decay.* The decay kinetics of the excited singlet state of P are complex, having components on the picosecond to nanosecond time scale in reaction centers where electron transfer to the quinone is blocked. One way to explain the complex kinetics of P* decay in reaction centers is in terms of a static conformational distribution of reaction centers, each with a different P/P^+ midpoint potential. Such a heterogeneity in midpoint potential might give rise to a heterogeneity both in the forward electron-transfer rate and in the charge recombination rate. However, the weak dependence of the forward electron-transfer rate on the P/P^+ midpoint (roughly a factor of 20 over a 350 mV range *22*) suggests that a moderate distribution of midpoint potentials would have only minor effects on the initial electron-transfer rate (for example, a 100 meV increase in the P/P^+ midpoint potential changes the forward charge separation rate by only about a factor of 2; *22*). The data in Figure 3 show that the recombination rate of $P^+H_A^-$ is even less dependent on the P/P^+ potential. This makes it very unlikely that heterogeneity in the P* decay arises from equilibration between this state and a distribution of $P^+H_A^-$ states that have different lifetimes due to a distribution of P/P^+ midpoint potentials. Of course, this does not rule out distributions in the midpoints potentials of B_A and/or H_A as playing an important role in the complex kinetics. It is also likely that a large aspect of the kinetic complexity of P* decay arises from time-dependent relaxation of charge-separated states, as discussed in the introduction. Thus, any reaction center heterogeneity that affects the rates of forward electron transfer and $P^+H_A^-$ recombination must arise from parameters other than the P/P^+ midpoint potential, such as the relative energies of B^- and H^- or distributions in the electronic coupling between excited and charge-separated states.

ACKNOWLEDGMENT

We acknowledge Kristina Schneider and Kathryn Strain for assistance in sample preparation.

REFERENCES

1. Woodbury, N. W., and Allen, J. P. (1995) in *Anoxygenic Photosynthetic Bacteria* (Blankenship, R. E., Madigan, M. T., and Bauer, C. E., Eds.) Vol. 2, pp 527−557, Kluwer Academic Publishers, Dordrecht, The Netherlands.
2. Zinth, W., and Kaiser, W. (1993) in *The Photosynthetic Reaction Center* (Deisenhofer, J., and Norris, J. R., Eds.) Vol. II, pp 71−88, Academic Press, San Diego, CA.
3. Parson, W. W. (1987) in *Photosynthesis* (Amesz, J., Ed.) pp 43−61, Elsevier, Amsterdam.
4. Martin, J.-L., and Vos, M. H. (1992) *Annu. Rev. Biophys. Biomol. Struct. 21*, 199−222.
5. Kirmaier, C., and Holten, D. (1993) in *The Photosynthetic Reaction Center*, (Deisenhofer, J., and Norris, J. R., Eds.) Vol. II, pp 49−70, Academic Press, San Diego, CA.
6. Kirmaier, C., and Holten, D. (1987) *Photosynth. Res. 13*, 225−260.
7. Feher, G., Allen, J. P., Okamura, M. Y., and Rees, D. C. (1989) *Nature 339*, 111−116.
8. Schenck, C. C., Blankenship, R. E., and Parson, W. W. (1982) *Biochim. Biophys. Acta 680*, 44−59.
9. Woodbury, N. W. T., and Parson, W. W. (1984) *Biochim. Biophys. Acta 767*, 345−361.
10. Williams, J. C., Alden, R. G., Murchison, H. A., Peloquin, J. M., Woodbury, N. W., and Allen, J. P. (1992) *Biochemistry 31*, 11029−11037.
11. Peloquin, J. M., Williams, J. C., Lin, X., Alden, R. G., Murchison, H. A., Taguchi, A. K. W., Allen, J. P., and Woodbury, N. W. (1994) *Biochemistry 33*, 8089−8100.
12. Müller, M. G., Griebenow, K., and Holzwarth, A. R. (1992) *Chem. Phys. Lett. 199*, 465−469.
13. Hartwich, G., Lossau, H., Michel-Beyerle, M. E., and Ogrodnik, A. (1998) *J. Phys. Chem. B 102*, 3815−3820.
14. Du, M., Rosenthal, S. J., Xie, X., DiMagno, T. J., Schmidt, M., Hanson, D. K., Schiffer, M., Norris, J. R., and Fleming, G. R. (1992) *Proc. Natl. Acad. Sci. U.S.A. 89*, 8517−8521.
15. Stanley, R. J., and Boxer, S. G. (1995) *J. Phys. Chem. 99*, 859−863.
16. Booth, P. J., Crystall, B., Giorgi, L. B., Barber, J., Klug, D. R., and Porter, G. (1990) *Biochim. Biophys. Acta 1016*, 141−152.
17. Konermann, L., Gatzen, G., and Holzwarth, A. R. (1997) *J. Phys. Chem. B 101*, 2933−2944.
18. Müller, M. G., Drews, G., and Holzwarth, A. R. (1993) *Biochim. Biophys. Acta 1142*, 49−58.
19. Woodbury, N. W., Peloquin, J. M., Alden, R. G., Lin, X., Lin, S., Taguchi, A. K. W., Williams, J. C., and Allen, J. P. (1994) *Biochemistry 33*, 8101−8112.
20. Ogrodnik, A., Keupp, W., Volk, M., Aumeier, G., and Michel-Beyerle, M. E. (1994) *J. Phys. Chem. 98*, 3432−3439.
21. Holzwarth, A. R., and Müller, M. G. (1996) *Biochemistry 35*, 11820−11831.
22. Allen, J. P., and Williams, J. C. (1995) *J. Bioenerg. Biomembr. 27*, 275−283.
23. Volk, M., Aumeier, G., Langenbacher, T., Feick, R., Ogrodnik, A., and Michel-Beyerle, M.-E. (1998) *J. Phys. Chem. B 102*, 735−751.
24. Volk, M., Neumann, W., Ogrodnik, A., Gray, K. A., Oesterhelt, D., and Michel-Beyerle, M.-E. (1993) *Biophys. J. 64*, A18.
25. Ogrodnik, A., Friese, M., Gast, P., Hoff, A. J., and Michel-Beyerle, M.-E. (1996) *Biophys. J. 70*, A142.
26. Paddock, M. L., Rongey, S. H., Feher, G., and Okamura, M. Y. (1989) *Proc. Natl. Acad. Sci. U.S.A. 86*, 6602−6606.

27. Lin, X., Murchison, H. A., Nagarajan, V., Parson, W. W., Allen, J. P., and Williams, J. C. (1994) *Proc. Natl. Acad. Sci. U.S.A. 91*, 10265−10269.
28. Okamura, M. Y., Isaacson, R. A., and Feher, G. (1975) *Proc. Natl. Acad. Sci. U.S.A. 72*, 3491−3495.
29. Farhoosh, R., Chynwat, V., Gebhard, R., Lugtenburg, J., and Frank, H. A. (1997) *Photochem. Photobiol. 66*, 97−104.
30. Frank, H. A., Chynwat, V., Posteraro, A., Hartwich, G., Simonin, I., and Scheer, H. (1996) *Photochem. Photobiol. 64*, 823−831.
31. Robles, S. J., Breton, J., and Youvan, D. C. (1990) *Science 248*, 1402−1405.
32. Nagarajan, V., Parson, W. W., Gaul, D., and Schenck, C. C. (1990) *Proc. Natl. Acad. Sci. U.S.A. 87*, 7888−7892.
33. Nagarajan, V., Parson, W. W., Davis, D., and Schenck, C. C. (1993) *Biochemistry 32*, 12324−12336.
34. Marcus, R. A. J. (1956) *Chem. Phys. 24*, 966.
35. Bixon, M., and Jortner, J. (1991) *J. Phys. Chem. 95*, 1941−1944.
36. Marcus, R. A., and Sutin, N. (1985) *Biochim. Biophys. Acta 811*, 265−322.
37. Kirmaier, C., Gaul, D., DeBey, R., Holten, D., and Schenck, C. C. (1991) *Science 251*, 922−927.
38. Deisenhofer, J., Epp, O., Miki, K., Huber, R., and Michel, H. (1984) *J. Mol. Biol. 180*, 385−398.
39. Deisenhofer, J., Epp, O., Miki, K., Huber, R., and Michel, H. (1985) *Nature 318*, 618−624.
40. Allen, J. P., Feher, G., Yeates, T. O., Komiya, H., and Rees, D. C. (1987) *Proc. Natl. Acad. Sci. U.S.A. 84*, 5730−5734.
41. Allen, J. P., Feher, G., Yeates, T. O., Komiya, H., and Rees, D. C. (1988) *Proc. Natl. Acad. Sci. U.S.A. 85*, 8487−8491.
42. Chang, C.-H., El-Kabbani, O., Tiede, D., Norris, J., and Schiffer, M. (1991) *Biochemistry 30*, 5352−5360.
43. El-Kabbani, O., Chang, C.-H., Tiede, D., Norris, J., and Schiffer, M. (1991) *Biochemistry 30*, 5361−5369.
44. Ermler, U., Fritzsch, G., Buchanan, S. K., and Michel, H. (1994) *Structure 2*, 925−936.

BI990346Q